A land surface model combined with a crop growth model for paddy rice (MATCRO-Rice Ver. 1) – Part II: Model validation

Yuji Masutomi[1], Keisuke Ono[2], Takahiro Takimoto[3], Masayoshi Mano[4], Atsushi Maruyama[2], and Akira Miyata[2]

[1]College of Agriculture, Ibaraki University, 3-21-1, Chuo, Ami, Inashiki, Ibaraki 300-0393, Japan
[2]Intstitute for Agro-Environmental Sciences, National Agriculture and Food research Organization, 3-1-3, Kannondai, Tsukuba, Ibaraki 305-8604, Japan
[3]Institute for Global Change Adaptation Science, Ibaraki University, 3-21-1, Chuo, Ami, Inashiki, Ibaraki 300-0393, Japan
[4]Graduate School of Horticulture, Chiba University, 648 Matsudo, Matsudo-shi, Chiba 271-8510, Japan

Correspondence to: Yuji Masutomi (yuji.masutomi@gmail.com)

Abstract. We conducted two types of validations for the simulations by MATCRO-Rice developed by Masutomi et al. (2016). In the first validation, we compared simulations with observations for latent heat flux (LHF), sensible heat flux (SHF), net carbon uptake by crop, and paddy rice yield from 2003 to 2006 at the site where model parameters are parameterised. In the second validation, we compared the observed and simulated paddy rice yields over Japan from 1991 to 2010 between observations and simulations. The 4-year average root mean square errors (RMSEs) of the first validation for LHF and SHF were 18.20 and 15.47 W m^{-2}, respectively. These values for errors are comparable to those reported in earlier studies. The comparison of biomass growth during growing periods from 2003 to 2006 at the parameterisation site shows that the simulations were in agreement with the observations, indicating that the model can reproduce the net carbon uptake by crop well. The 4-year average RMSE of the first validation for crop yield in the same period was 410.6 kg ha^{-1}, which accounted for 8.1% of the mean observed yields. The error of the second validation for crop yield was 18.8% and the correlation of crop yields between observations and simulations from 1991 to 2010 was significant at 0.671 (P<0.01). These results indicate that MATCRO-Rice has high ability to accurately and consistently simulate LHF, SHF, net carbon uptake by crop, and crop yield.

1 Introduction

It has been recognized that crop growth and management in agricultural land are important factors that affect climate at various spatial and temporal scales via exchange of heat, water, and gases (Tsvetsinskaya et al., 2001;Bondeau et al., 2007; Osborne et al., 2009; Levis et al., 2012). Betts (2005) pointed out that integration of crop growth models (CGMs) into climate models is needed for accurate climate simulations by climate models. To consider the influence of agricultural land on climate in climate simulations, several land surface models (LSMs) or dynamics vegetation models (DVMs) incorporated with a CGM have been developed (Tsvetsinskaya et al., 2001; Kucharik, 2003; Gervois et al., 2004; Bondeau et al., 2007; Osborne et al., 2007; Lokupitiya et al., 2009; Maruyama and Kuwagata, 2010; Levis et al., 2012; Osborne et al., 2015).

Masutomi et al. (2016) have developed a new LSM-CGM combined model, called MATCRO-Rice, by incorporating a CGM into a LSM, MATSIRO (Takata et al., 2003). The most important feature of the model is that it can consistently simulate latent heat flux (LHF), sensible heat flux (SHF), net carbon uptake by crop, and crop yield in paddy rice fields by exchanging variables between an LSM and a CGM. The consistency among model outputs enable us to apply the model to a wide range of integrated issues. For example, the model can investigate the interaction between climate and paddy rice fields, consistently considering impacts of climate on rice productivity and impacts of paddy rice fields on climate. Osborne et al. (2009) showed that this interaction can affect variability in climate and crop production. Therefore, the understanding of the interaction is important for securing food security. However, little is known about the interaction. MATCRO-Rice can be a useful tool to study the interaction between climate and paddy rice fields.

The objective of the present paper is to present the results of the comprehensive validation of MATCRO-Rice and to show the effects of modifications from the original LSM, MATSIRO. Before presenting the results of the validation and the effects of modification, we first show the numerical method (Section 2) and the method and results of parameterisation for model parameters (Section 3). The results of model validation and the effects of modifications are shown in Sections 4 and 5, respectively, followed by concluding remarks in Section 6

2 Numerical setting and method

All simulation setting parameters are shown in Table 1. We set the time resolution of the simulation to half hour, i.e., $\delta_t = 1800$. For time discretisation, the forward difference method was used.

To simulate soil water and heat transfer (Section 3.5 in Masutomi et al. (2016)), we spatially discretised soil into five layers with thickness of 0.05, 0.2, 0.75, 1.0, and 2.0 m, resulting in $z_{\max} = 4.0$ m, $z_{\mathrm{t}} = 0.05$ m, and $z_{\mathrm{b}} = 2.0$ m. To simulate soil water content for each soil layer (w_{s}), we replaced the gradient of water flux by net water fluxes between layers. In the calculation for water fluxes between layers, we used the hydraulic conductivity that is smaller among soil layers and the difference in water potentials between soil layers. After the calculation for soil water content for each layer, water content beyond saturation was taken out to base flow.

To simulate soil temperature for each soil layer, we solved the system of equations for soil layers by using the Gauss-Jordan method. In the calculation of soil temperatures, we replaced the gradient of heat flux by net heat fluxes between layers. In the calculation of heat fluxes between layers, we used thermal conductivity averaged between soil layers and soil temperatures for each layer.

The downhill simplex method (Nelder and Mead, 1965) was used to simulate temperatures of the canopy and surface (T_{c} and T_{g}; Section 3.1 in Masutomi et al. (2016)), bulk transfer coefficients (C_{Eg}, C_{Ec}, C_{Hg}, C_{Hc}, C_{M}, and C_{Mg}; Section 3.3 in Masutomi et al. (2016)), and variables related to carbon assimilation ($\overline{A}_{\mathrm{n},x}, c_{\mathrm{i},x}$, and $\overline{g}_{\mathrm{st},x}$; Section 4.1 in Masutomi et al. (2016)) .

We set $z_{\mathrm{a}} = 3$. CO_2 concentration ($C_{\mathrm{a,ppm}}$) and the depth of surface water (d_{w}) were set at 390 ppm and 0.025 m, respectively. The initial dry weight of each organ was set at 1 kg ha^{-1} for leaf ($W_{\mathrm{lef},0}$), stem ($W_{\mathrm{stm},0}$), and root ($W_{\mathrm{rot},0}$) and at 0.5 kg ha^{-1} for glucose reserve in leaf ($W_{\mathrm{glu},0}$).

$D_{\mathrm{oy,Ie}}$, $D_{\mathrm{oy,Is}}$, $D_{\mathrm{oy,sw}}$, and L_{t} depend on the simulations. Values for these parameters are shown in the sections of each simulation.

3 Parameterisation

Table 2 shows model parameters parameterised in the present paper. All parameters are parameterised using observations, the literature, and assumptions. The method of the parameterisation is explained in this section.

3.1 Parameterisation site and observation data

Table 3 shows the observational data used for parameterisation. The data were observed from 2003 to 2006 at a site which is located in Tsukuba, Japan (Lat: 36° 03' 14.3" N; Lon: 140° 01' 36.9" E), at 13 m above sea level. The climatic zone of the site is temperate, with the mean annual air temperature 13.7°C and precipitation 1200 mm. The soil type is clay loam. The variety planted at the site is "Koshihikari", which is the most planted variety in Japan.

Biomass for each organ (W_{lef}, W_{pnc}, W_{rot}, and W_{stm}) and leaf area index (L) were measured nearly every two weeks. At each measuring time, ten stands were sampled from the fields. Yield (Y_{ld}) and phenological dates including transplanting ($D_{\mathrm{oy,tr}}$), heading ($D_{\mathrm{oy,hd}}$), and harvest ($D_{\mathrm{oy,hv}}$) were observed every year. The values of observed yield are the husked rice yield with 15% water content. The rice grains for measuring yield were sampled from the whole fields of the observational site. The crop height (h_{gt}) was measured on average every 5 days.

3.2 Phenology

Phenological parameters that represent development stages ($D_{\mathrm{vs,e}}$, $D_{\mathrm{vs,h}}$, $G_{\mathrm{ds,m}}$, $D_{\mathrm{vs,tr}}$, and $D_{\mathrm{vs,te}}$) were parameterised. First, we calculated D_{vs}s at heading and $G_{\mathrm{ds,m}}$s from 2003 to 2006 using the phenological model given by Masutomi et al. (2016). The mean values were set to $D_{\mathrm{vs,h}}$ and $G_{\mathrm{ds,m}}$, resulting in $D_{\mathrm{vs,h}} = 0.616$ and $G_{\mathrm{ds,m}} = 167759940$. Figure 1 compares the heading and harvest dates between observations and simulations from 2003 and those from 2006. The simulated heading and harvest dates were in good agreement with the observations. The average errors were 2.25 and 4.5 days for heading and harvest, respectively.

$D_{\mathrm{vs,e}}$, $D_{\mathrm{vs,tr}}$, and $D_{\mathrm{vs,te}}$ were determined so that the duration from sowing to emergence, transplanting, and the end of transplanting shock was 5, 20, and 25 days, respectively. Thus, $D_{\mathrm{vs,e}} = 0.012$, $D_{\mathrm{vs,tr}} = 0.06$, and $D_{\mathrm{vs,te}} = 0.08$.

3.3 Partitioning

Parameters related to glucose partitioning ($D_{\mathrm{vs,rot1}}$, $D_{\mathrm{vs,rot2}}$, $D_{\mathrm{vs,lef1}}$, $D_{\mathrm{vs,lef2}}$, $D_{\mathrm{vs,pnc1}}$, $D_{\mathrm{vs,pnc2}}$, P_{rot}, and P_{lef}) were parameterised as follows: (i) we calculated the ratio of glucose partitioned to each organ (leaf, stem, root, panicle) during the

growing period using the observed biomass for each organ; (ii) we conducted the curve fitting of the calculated ratios in (i). Figure 2 shows the calculated ratios of glucose partitioned to each organ and the fitting curves for the ratios.

To determine the ratio of dead leaf at harvest ($r_{\mathrm{d1,lef}}$), we first calculated the observational ratios of dead leaf during growing period by dividing the decrease in leaf biomass between observational dates by the duration among the observational dates. Then by graphically fitting a curve to the calculated ratios of dead leaf, we determined $r_{\mathrm{d1,lef}}$. Figure 3 shows the calculated ratios of dead leaf and the fitted curve.

The fraction of glucose allocated to starch reserve (f_{stc}) is determined as follows: (i) we first calculated the ratios of stem biomass at harvest to maximum stem biomass for each year from 2003 to 2006 (Bouman et al. (2001)); (ii) then, a 4-year average was calculated for f_{stc}.

3.4 LAI, crop height, and specific leaf weight

To obtain the parameters for the relationship between LAI and crop height ($h_{\mathrm{aa}}, h_{\mathrm{ab}}, h_{\mathrm{ba}}$, and h_{bb}), we conducted linear regressions of the data before and after heading using observations for LAI and crop height from 2003 to 2006. Thus, $h_{\mathrm{aa}} = 0.439, h_{\mathrm{ab}} = 0.675, h_{\mathrm{ba}} = 0.366$, and $h_{\mathrm{bb}} = 0.318$. Figure 4 compares the LAI–height relation between observations and simulations.

To obtain parameters for specific leaf weight ($k_{\mathrm{S_{lw}}}, S_{\mathrm{lw,mn}}$, and $S_{\mathrm{lw,mx}}$), we plotted observations for specific leaf weights during growing periods from 2003 to 2006 and conducted the curve fitting of the plotted data. Thus, $k_{\mathrm{S_{lw}}} = 3.5, S_{\mathrm{lw,mn}} = 350$, and $S_{\mathrm{lw,mx}} = 600$. Figure 5 shows the specific leaf weights and the fitted curve.

3.5 Crop yield

To determine the ratio of crop yield to dry weight of panicle at harvest (k_{yld}), we calculated the dry weight of panicle at harvest, because the weight was not observed. By assuming linear increase of dry weight from the last date in which dry weight of the panicle was measured, we calculated the dry weight of the panicle at harvest from 2003 to 2006. The median value among the ratios of observed yields to the calculated dry weight of panicle produced k_{yld}.

3.6 Rubisco-limited photosynthesis rate

Parameters related to Rubisco-limited photosynthesis rate ($V_{\mathrm{max}}(0)$, s_1, and s_2) were parameterised using the values obtained from the literature. In this parameterisation, we adjusted the parameters so that the Rubisco-limited photosynthesis rate ($\overline{\omega}_{\mathrm{c},x}$) simulated by MATCRO agrees with the observational value reported by Borjigidai et al. (2006). In the simulations, CO_2 concentration in the leaf was fixed to $c_{\mathrm{i},x} = 30$ Pa. Figure 6, showing the comparison of Rubisco-limited photosynthesis rates among MATCRO, those reported by Borjigidai et al. (2006), and MATSIRO (Takata et al., 2003), on which MATCRO is based, indicate that there is a good agreement in the photosynthesis rate between the simulations of MATCRO and the observational value in Borjigidai et al. (2006); the simulations for the photosynthesis rate of MATCRO were significantly improved compared to those of MATSIRO.

4 Validation

We conducted two types of validation. The first validation was conducted at the parameterisation site as explained in Section 3.1. In the validation, the simulated LHF, SHF, carbon uptake by crop, and crop yields were compared with the observations from 2003 to 2006.

The second validation was conducted for a territory across Japan. The simulated crop yield for the area from 31°N to 38°N in Japan, which corresponds to 73% of all area under rice cultivation in Japan, was compared with the national statistics from 1991 to 2010. The area at higher latitudes than 38°N was excluded in the validation, because the crop yields simulated by MATCRO were often zero at that area due to low temperatures. We also excluded the area at lower latitude than 31°N, because the cropping system at that area is different from that employed in other areas in Japan due to high temperatures.

4.1 Validation at the parameterisation site

4.1.1 Input and validation data

Table 4 shows the observational data used for the validation. Information on the instruments used for the observations are available from the AsiaFlux web site (AsiaFlux, 2016). The height at which the wind speed was measured was different each year. Assuming logarithmic vertical profile of the wind, we transformed the observed wind speed to that at 3 m above ground, because the reference height ($z_{\rm a}$) is set to be 3m (Section 3.1). It is noted that we used the observed values of photosynthesis active radiation (PAR) in addition to the standard meteorological inputs, because PAR, which is often not measured, was observed at the parameterisation site. We set $L_{\rm t} = 36.05$. Values for soil parameters for clay loam are shown in Table 5. The "Koshihikari" variety was planted using a transplanting technique. We set $D_{\rm oy,Is}$=114, 107, 114, 113, and $D_{\rm oy,Ie}$=231, 251, 243, 241 from 2003 to 2006, respectivey, using the observations for the depth of surface water ($d_{\rm wo}$). $D_{\rm oy,sw}$ was calculated from the observed transplanting date ($D_{\rm oy,tr}$), assuming that transplanting was conducted 20 days after sowing, i.e., $D_{\rm oy,sw} = D_{\rm oy,tr} - 20$.

The validation was conducted from 2003 to 2006, although the AsiaFlux provides the observational data from 2001 to 2006 for the site. We did not use the observational data before 2002 because the flux tower was relocated in the paddy fields in April 2003. Thereafter, the observed flux data have been more representative of the field, where the rice sampling was conducted.

4.1.2 Comparison of LHF and SHF

Figures 7 to 10 show the comparison of the daily and half-hourly LHF and SHF from 2003 to 2006. We can observe that MATCRO can replicate the daily and half-hourly variations in LHF and SHF accurately. Quantitatively, the RMSEs of daily LHF between simulations and observations for each year were 15.15, 21.84, 17.25, and 18.57 W m^{-2}, with the 4-year average of 18.20 W m^{-2}. The RMSEs of daily SHF were 13.62, 14.72, 14.84, and 18.69 W m^{-2}, with the 4-year average of 15.47 W m^{-2}. These RMSE values are comparable to those reported in earlier studies (Kimura and Kondo,1998; Maruyama and Kuwagata,2010).

One of the major reasons for the errors of LHF and SHF between simulations and observations is thought to be a problem in flux observations. Aubinet et al. (2000) reported that the energy balance in observations is not closed. In contrast, the energy balance simulated by MATCRO is completely closed. Therefore, the energy imbalance in flux observations can cause errors between simulations and observations. El Maayar et al. (2008) suggested to test the degree of energy imbalance in observations before comparing the observations with simulations. This degree is generally evaluated by

$$I_{\mathrm{m}} = \left(\sum_{d} \frac{(\overline{H}(d) + \lambda \overline{E}(d))}{(\overline{R}_{\mathrm{n}}(d) - \overline{G}(d))} \right) / N, \tag{1}$$

where $\overline{H}$, $\lambda\overline{E}$, $\overline{R}_{\mathrm{n}}$, and $\overline{G}$ are the daily averages for SHF, LHF, net radiation, and heat flux into ground, respectively, d indicates a day, and N is the number of days. The observation values for R_{n} and G in this equation are expected to be sufficiently accurate (Twine et al., 2000; Wilson et al., 2002). The values of I_{m} in the observations from 2003 to 2006 were 0.79, 0.77, 0.78, and 0.74, with the average of 0.78. In other words, these results imply that the total flux of observed LHF and SHF can be smaller than a true value. The ratio of the total flux of observed LHF and SHF to that of simulated LHF and SHF from 2003 to 2006 were 0.84, 0.79, 0.80, and 0.83, with the average of 0.82. This suggests that the errors of LHF and SHF between observations and simulations can be largely attributed to the energy imbalance in observations.

4.1.3 Comparison of net carbon uptake by crop

In this section, we tested the accuracy of MATCRO for simulating net carbon uptake by crop during growing periods by comparing the changes in total biomass between simulations and observations. Figure 11 compares the growth of the total biomass between simulations and observations from 2003 to 2006. As indicated by the figure, the simulated total biomass was in good agreement with the observations. Hence, we conclude that the model has high accuracy for simulating net carbon uptake by crop during growing period.

4.1.4 Comparison of yield

Figure 12 shows the comparison of the observed and simulated yields from 2003 to 2006. As indicated by the figure, MATCRO can reproduce well the absolute values of crop yields. The mean RMSE from 2003 to 2006 was 410.6 kg ha^{-1}, which was 8.1% of the mean observed yields. However, the model overestimated the crop yields in 2003. The primary cause of the large overestimation in 2003 can be attributed to the late harvest in the simulation for 2003; the model delayed the harvest by 11 days in 2003 (see Section 3.2). To confirm this, we recalculated the yield in 2003 by using the observed harvest date. The revised yield is shown in the figure as a red circle. The revised yield was in good agreement with the observations in 2003. These results suggest that the phenological model in MATCRO should be further improved for a more accurate estimation of crop yield. The current version of the phenological model in MATCRO implements only the temperature. The consideration of the photoperiod may further improve the accuracy of the phenological model in the simulation of harvest date as well as heading date (e.g., Penning de Vries et al., 1989; Connor et al. ,2011).

4.2 Validation over Japan

4.2.1 Input and validation data

Global Meteorological Forcing Dataset for land surface modelling (Sheffield et al., 2006) was used for meteorological input data. Because the spatial resolution of the input data is 1 degree, we simulated crop yields at the spatial resolution of 1 degree. The simulation settings and parameters for crop and soil were set using the values shown in Tables 1, 2, and 5. Because the time resolution of the input data is 3 hours, we used the same values at each 3 hours for half-hourly simulations. We set $D_{\mathrm{oy,tr}} = 100$, $D_{\mathrm{oy,Is}} = 1$ and $D_{\mathrm{oy,Ie}} = 365$. L_{t} was set to the latitude of the center of each grid. After averaging the crop yields simulated at all grids, we compared the averaged crop yields with the national crop yields reported by FAOSTAT (http://faostat.fao.org/).

4.2.2 Comparison of yield

Figure 13 shows the comparison of the observed and simulated yields from 1991 to 2010. The average error between simulations and observations was 18.8%. The simulated yields were overestimated for all simulation years. The correlation between simulations and observations was significant at 0.671(P<0.01). Hence, we conclude that MATCRO can reproduce annual variability of yields correctly.

5 Effects of modifications

There are two major modifications of MATCRO from the original LSM (MATSIRO). The first one is the dynamic calculation of LAI, crop height, and root. The other is the consideration of flooded surface and irrigation. We quantify the effects of the two major modifications on the simulation of LHF and SHF. Both simulations are conducted at the parameterisation site from 2003 to 2006 (Section 3.1).

5.1 Effect of dynamic calculation of LAI

The original LSM (MATSIRO) uses the monthly constant LAI, which is given in grids by grids. The default gridded LAI data of MATSIRO were obtained from the Global Soil Wetness Project 2 (Dirmeyer et al., 2006). Figure 14 shows the comparison of LAI between observations, simulations by MATCRO, and the default values of MATSIRO. We can see that MATCRO reproduces adequately seasonal changes in LAI well, although the default LAI are not in agreement with the observed LAI. MATSIRO also uses constant crop height and root length, which are vegetation-specific parameters. The default values of crop height and root length for crops are 1m. Using the default data for LAI and the default values for crop height and root length, we simulated LHF and SHF from 2003 to 2006. In the simulations, we also used the original equation for the maximum canopy water ($w_{\mathrm{cap}} = 0.002L$), because MATSIRO does not calculate the shoot weight (W_{sh}) used for the calculation of w_{cap} in MATCRO.

The RMSEs of daily LHF from 2003 to 2006 were 19.4, 20.78, 19.28, and 18.72 W m^{-2}, respectively, with the 4-year average of 19.54 W m^{-2}. The RMSEs of daily SHF from 2003 to 2006 were 14.69, 20.30, 16.93, 20.68 W m^{-2}, respectively,

with the 4-year average of 18.15 W m^{-2}. These errors are compatible to those of MATCRO. Hence, we conclude that the effects of the dynamic calculation of LAI, crop height and root length on LHF and SHF are small.

5.2 Effect of flooded and irrigated surface

We simulated LHF and SHF from 2003 to 2006 without flooded surface and irrigation. The simulations are called MATCRO-RF. Figures 15 and 16 show the comparison of daily LHF and LHF between observations and simulations obtained by MATCRO and MATCRO-RF. The LHF and SHF simulated by MATCRO-RF were not in agreement with the observations. The RMSEs of daily LHF simulated by MATCRO-RF from 2003 to 2006 were 16.63, 36.90, 29.32, and 24.93 W m^{-2}, respectively, with the 4-year average of 26.95 W m^{-2}. The RMSEs of daily SHF from 2003 to 2006 were 16.34, 42.02, 34.16, 31.56 W m^{-2}, respectively, with the 4-year average of 31.02 W m^{-2}. These errors in MATCRO-RF are considerably larger than those simulated by MATCRO. To identify the cause of the large errors of the LHF and SHF simulated by MATCRO-RF, we compared surface temperature between observations and simulations obtained by MATCRO and MATCRO-RF. Figure 17 shows the comparison of surface temperature. MATCRO reproduces the observations of surface temperature correctly, while MATCRO-RF tends to overestimate the observations. The RMSEs of surface temperature simulated by MATCRO were 1.95, 1.41, 1.18 1.20 K, respectively, with the 4-year average of 1.44 K, while those simulated by MATCRO-RF were 1.24, 3.31, 2.60, 2.05, respectively, with the 4-year average of 2.32 K. Therefore, the large errors of the LHF and SHF simulated by MATCRO-RF can be attributed to the overestimation of surface temperature simulated by MATCRO-RF. Hence, we conclude that the flooded surface and irrigation have large effects on the simulations of LHF and SHF.

6 Concluding remarks

In this paper, we presented the results of the validation of MATCRO-Rice and the effects of the modification of the original LSM (MATSIRO), and the numeric and parameterisation methods. First, the comparison of the LHF and SHF between simulations and observations at the paramerisation site confirmed that the model can reproduce the observed LHF and SHF data well. The accuracy of the simulations for LHF and SHF was comparable to those obtained in earlier studies. Second, we showed that the simulated growth of the total biomass was in good agreement with the observations at the parameterisation site. This indicates that the model can simulate the net carbon uptake by crop during a growing period at paddy rice fields. Last, we demonstrated that the model has high ability to simulate crop yield by comparing the simulated and observed yields at the parameterisation site and over Japan.

The validation results suggest that MATCRO-Rice has high ability to accurately and consistently simulate LHF, SHF, net carbon uptake by crop, and yield. There have been many models that simulate some of the four variables with high accuracy, but a few models can accurately and consistently simulate all four of them. This point is the most important feature of MATCRO-Rice. The model can be applied to a wide range of issues, including climate change impact (e.g., Masutomi et al.,2009), and it will facilitate the scientific research especially on the climate–crop interactions (Osborne et al.,2009).

We validated LHF, SHF, and carbon flux simulated by this model with observations from only one site. The model should be further validated at multiple sites in order to enforce the reliability and applicability of the model. However, since there are a few flux sites on agriculture land worldwide, it will be necessary to increase their number on agricultural land to promote climate–crop modelling studies.

We assessed the effects of the dynamics simulation of LAI, crop height and root length on LHF and SHF and the effect of flooded surface and irrigation on LHF and SHF. The results show that the effects of the dynamic simulation on LHF and SHF are small, whereas the flooded surface and irrigation have large effects on LHF and SHF. These results suggest that climate–crop modelling should incorporate flooded surface and irrigation.

7 Code availability

The source code of MATCRO will be distributed at request to the corresponding author (Yuji Masutomi: yuji.masutomi@gmail.com). The website for MATCRO-Rice will be developed in the near future.

Acknowledgements. We are grateful to Mrs Hatanaka for her help in extensive literature survey. This research was supported by the Environment Research and Technology Development Fund (S-12) and the Program on Development of Regional Climate Change Adaptation Plans in Indonesia (PDRCAPI) of the Ministry of the Environment.

References

AsiaFlux: MSE: Mase paddy flux site, http://asiaflux.net/index.php?page_id=83, Accessed on Feb. 5, 2016.

Aubinet, M., Grelle, A., Ibrom, A., Rannik, Ü., Moncrieff, J., Foken, T., Kowalski, A. S., Martin, P. H., Berbigier, P., Bernhoffer, Ch., Clement, R., Elbers, J., Granier, A., Grünwald, T., Morgenstern, K., Pilegaard, K., Rebmann, C., Snijders, W., Valentini, R., and Vesala, T.: Estimates of the annual net carbon and water exchange of forests: the EUROFLUX methodology. Adv. Ecol. Res., 30, 113-175, 1999.

Betts, R. A.: Integrated approaches to climate-crop modelling: needs and challenges, Phil. Trans. R. Soc. B, 360, 2049-2065, 2005.

Bondeau, A., Smith, P. C., Zaehle, S., Schaphoff, S., Lucht, W., Cramer, W., Gerten, D., Lotze-Campen, H., Müller, C., Reichstein, M., and Smith, B.: Modelling the role of agriculture for the 20th century global terrestrial carbon balance, Glob. Change Biol., 13, 679-706, 2007.

Borjigidai, A., Hikosaka, K., Hirose, T., Hasegawa, T., Okada, M., and Kobayashi, K.: Seasonal changes in temperature dependence of photosynthetic rate in rice under a free-air CO_2 enrichment, Ann. Bot., 97, 549-557, 2006.

Bouman, B. A. M., Kropff, M. J., Tuong, T. P., Wopereis, M. C. S., ten Berge, H. F. M., and van Laar, H. H.: ORYZA2000: modeling lowland rice, International Rice Research Institute and Wageningen University and Research Centre, Phillippines and Wageningen, 2001.

Campbell, G. S., and Norman, J. M.: An introduction to environmental biophysics, Springer-Verlag, New York, 1998.

Connor D. J., Loomis, R. S., and Cassman, K. G.: Crop ecology: productivity and management in agricultural systems, Cambridge University Press, Cambridge, 2011.

Dirmeyer, P. A., Gao, X., Zhao, M., Guo, Z., Oki, G., and Hanasaki, N.: GSWP-2, Multimodel analysis and implications for out perception of the land surface, Bull. Amer. Meteor. Soc., 87, 1381-1397, 2006.

Gervois, S., de Noblet-Ducoudré, N., Viovy, N., Ciais, P., Brisson, N., Seguin, B., and Perrier, A.: Including croplands in a global biosphere model: methodology and evaluation at specific sites, Earth Interact., 8, 1-25, 2004.

El Maayar, M., Chen, J. M., and Price, D. T.: On the use of field measurements of energy fluxes to evaluate land surface models, Ecol. Model., 214, 293-304, 2008.

Kimura, R., and Kondo, J.: Heat balance model over a vegetated area and its application to a paddy filed. J. Meteorol. Soc. Jpn., 76, 937-953, 1998.

Kucharik, C. J.: Evaluation of a process-based agro-ecosystem model (Agro-IBIS) across the U.S. corn belt: simulations of the interannual variability in maize yield, Earth Interact., 7, 1-33, 2003.

Lei, H., Yang, D., Lokupitiya, E., and Shen, Y.: Coupling land surface and crop growth models for predicting evapotranspiration and carbon exchange in wheat-maize rotation croplands, Biogeosciences, 7, 3363-3375, 2010.

Levis, S, Bonan, G. B., Kluzek, E., Thornton, P. E., Jones, A., Sacks, W. J., and Kucharik, C. J.: Interactive crop management in the Community Earth System Model (CESM1): Seasonal influences on land-atmosphere fluxes, J. Climate, 25, 4839-4859, 2012.

Lokupitiya, E., Denning, S., Paustian, K., Baker, I., Schaefer, K., Verma, S., Meyers, T., Bernacchi, C. J., Suyker, A., and Fischer, M.: Incorporation of crop phenology in Simple Biosphere Model (SiBcrop) to improve land-atmosphere carbon exchanges from croplands, Biogeosciences, 6, 969-986, 2009.

Maruyama, A., and Kuwagata, T.: Coupling land surface and crop growth models to estimate the effects of changes in the growing season on energy balance and water use of rice paddies, Agr. Forest Meteorol., 150, 919-930, 2010.

Masutomi, Y., Takahashi, K., Harasawa, H., and Matsuoka, Y.: Impact assessment of climate change on rice production in Asia in comprehensive consideration of process/parameter uncertainty in general circulation models, Agric. Ecosys. Environ., 131, 281-291, 2009

Masutomi, Y., Ono, Mano, M., Maruyama, A., and Miyata, A.: A land surface model combined with a crop growth model for paddy rice (MATCRO-Rice Ver. 1) – Part I: Model description, 2016 (submitted to Geosci. Model Dev. Discuss.)

Nelder, J. A., and Mead, R.: A simplex method for function minimization, Comput. J., 7, 308-313, 1965.

Oki, T., and Kanae, S.: Global hydrological cycles and world water resources, Science, 313, 1068-1072, 2006.

Osborne, T. M., Lawrence, D. M., Challinor, A. J., Slingo, J. M., and Wheeler, T. R.: Development and assessment of a coupled crop-climate model, Glob. Change Biol., 13, 169-183, 2007.

Osborne, T. M., Slingo, J., Lawrence, D., Wheeler, T.: Examining the interaction of growing crops with local climate using a coupled crop-climate model, J. Climate, 22, 1393-1411, 2009.

Osborne, T., Gornall, J., Hooker, J., Williams, K., Wiltshire, A., Betts, R., and Wheeler, T.: JULES-crop: a parametrisation of crops in the Joint UK Land Environment Simulator, Geosci. Model Dev., 8, 1139-1155, 2015.

Penning de Vries, F. W. T., Jansen, D. M., ten Berge, H. F. M., and Bakema, A.: Simulation of ecophysiological processes of growth in several annual crops, Centre for Agricultural Publishing and Documentation (Poduc), Wageningen, 1989.

Saxton, K. E., and Rawls, W. J.: Soil water characteristic estimates by texture and organic matter for hydrologic solutions. Soil Sci. Soc. Am. J. 70, 1569-1578, 2006.

Sheffield, J., Goteti, G., and Wood, E. F.: Development of a 50-yr high-resolution global dataset of meteorological forcings for land surface modelling, J. Climate , 19, 3088-3111, 2006.

Takata, K., Emori, S., and Watanabe, T.: Development of the minimal advanced treatments of surface interaction and runoff. Global Planet. Change, 38, 209-222, 2003.

Tsvetsinskaya, E. A., Mearns, L. O., and Easterling, W. E.: Investigating the effects of seasonal plant growth and development in three-dimensional atmospheric simulations. Part II: Atmospheric response to crop growth and development, J. Climate, 14, 711-729, 2001.

Twine, T. E., Kustas, W. P., Norman, J. M., Cook, D. R., Houser, P. R., Meyers, T. P., Prueger, J. H., Starks, P. J., and Wesely, M. L.: Correcting eddy-covariance flux underestimates over a grassland, Agr. Forest Meteorol., 103, 279-300, 2000.

Wilson, K. B., Baldocchi, D. D., Aubinet, M., Berbigier, P., Bernhofer, Ch., Dolman, H., Falge, E., Field, C., Goldstein, H., Granier, A., Grelle, A., Halldor, T., Hollinger, D., Katul, G., Law, B. E., Lindroth, A., Meyers, T., Moncrieff, J., Monson, R., Oechel, W., Tenhunen, J., Valentini, R., Verma, S., Vesala, T., and Wofsy, S.: Surface energy partitioning between latent and sensible heat flux at FLUXNET sites, Water Resour. Res., 38, 1294, 2002.

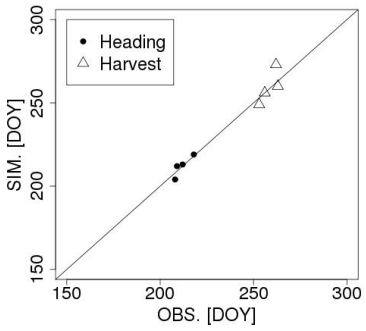

Figure 1. Comparison of heading and harvest dates. SIM: simulations; OBS: observations; DOY: The number of days from Jan. 1.

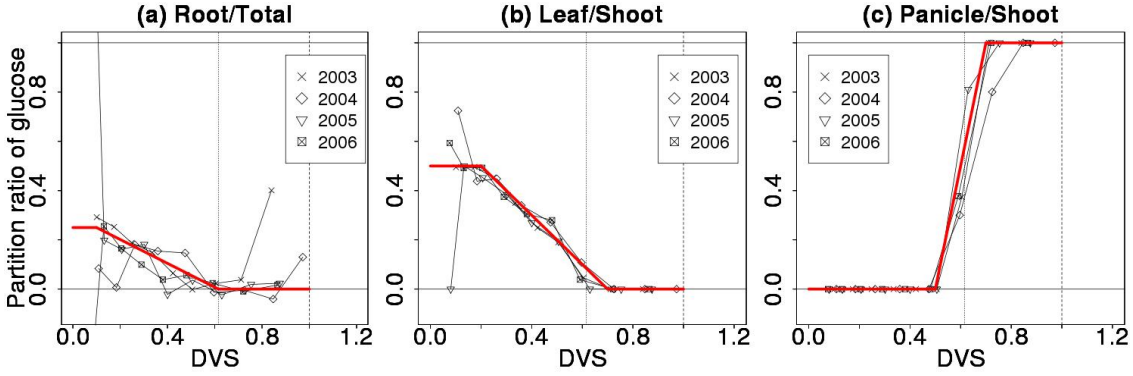

Figure 2. Partitioning ratio of glucose. Red lines are fitted. DVS: development stage

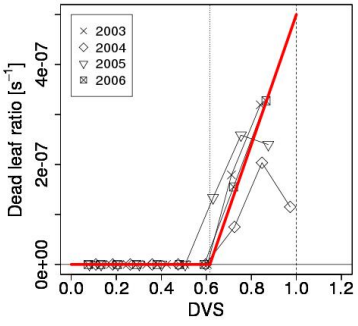

Figure 3. Ratio of dead leaf. DVS: development stage

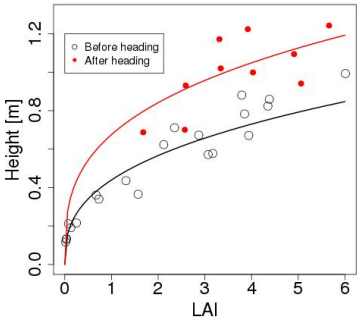

Figure 4. Relationship between the leaf area index (LAI) and crop height (black curve: $h_{\mathrm{gt}} = h_{\mathrm{aa}} L^{h_{\mathrm{ab}}}$; red curve: $h_{\mathrm{gt}} = h_{\mathrm{ba}} L^{h_{\mathrm{bb}}}$)

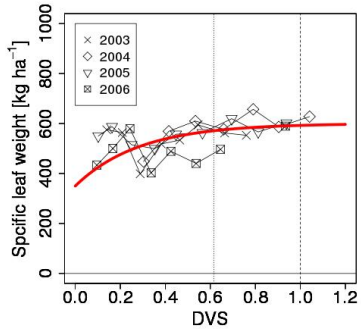

Figure 5. Relationship between specific leaf weight and development stage (DVS)

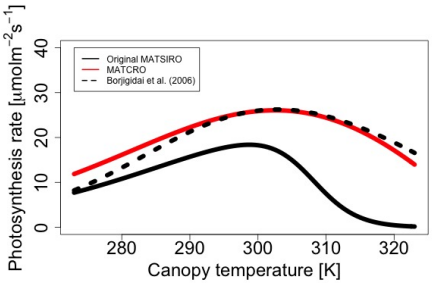

Figure 6. Rubisco-limited photosynthesis rate

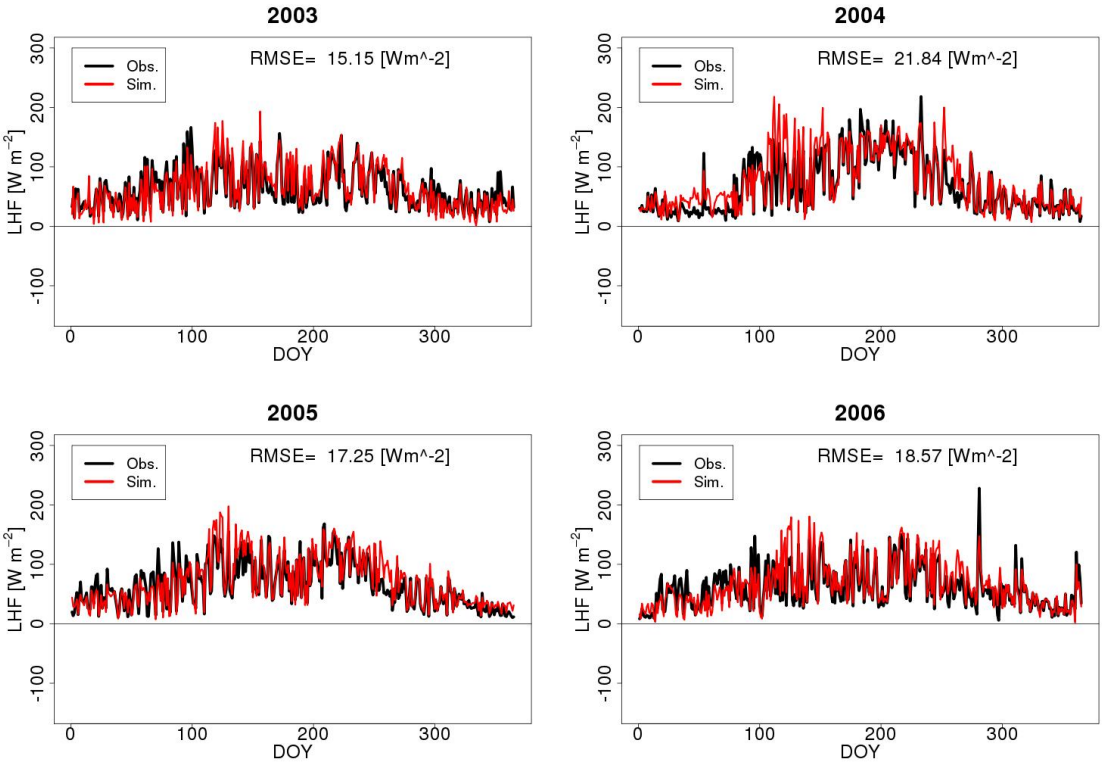

Figure 7. Comparison of daily latent heat flux (LHF) between simulations and observations. DOY: The number of days from Jan. 1.

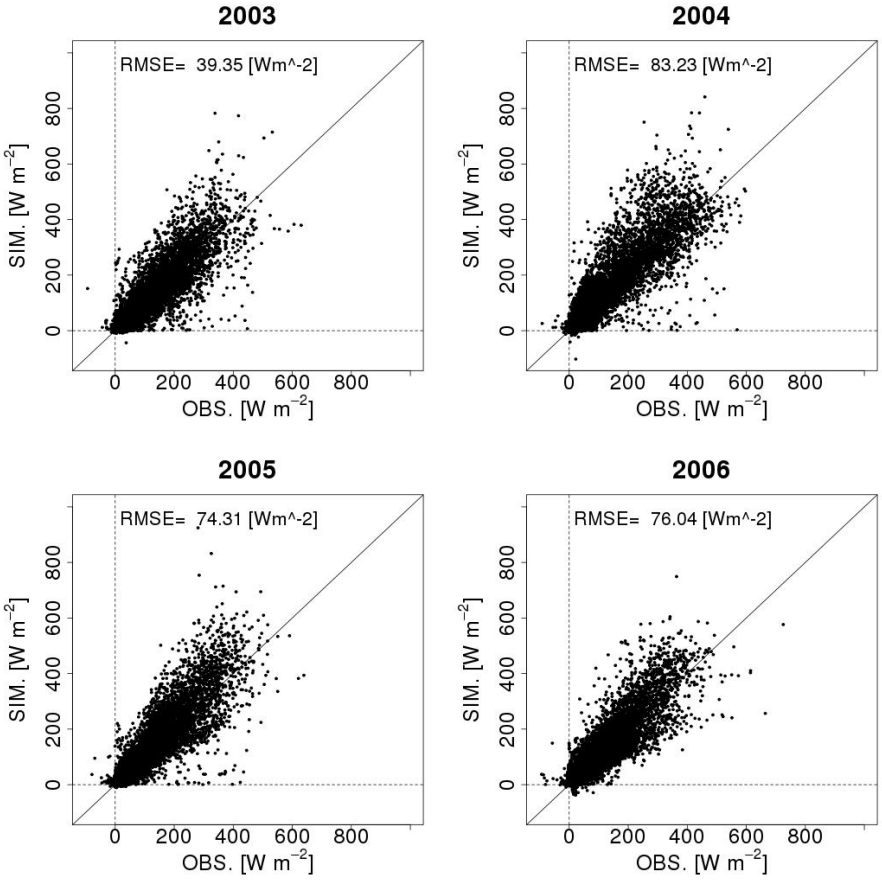

Figure 8. Comparison of half-hourly latent heat flux (LHF) between simulations and observations.

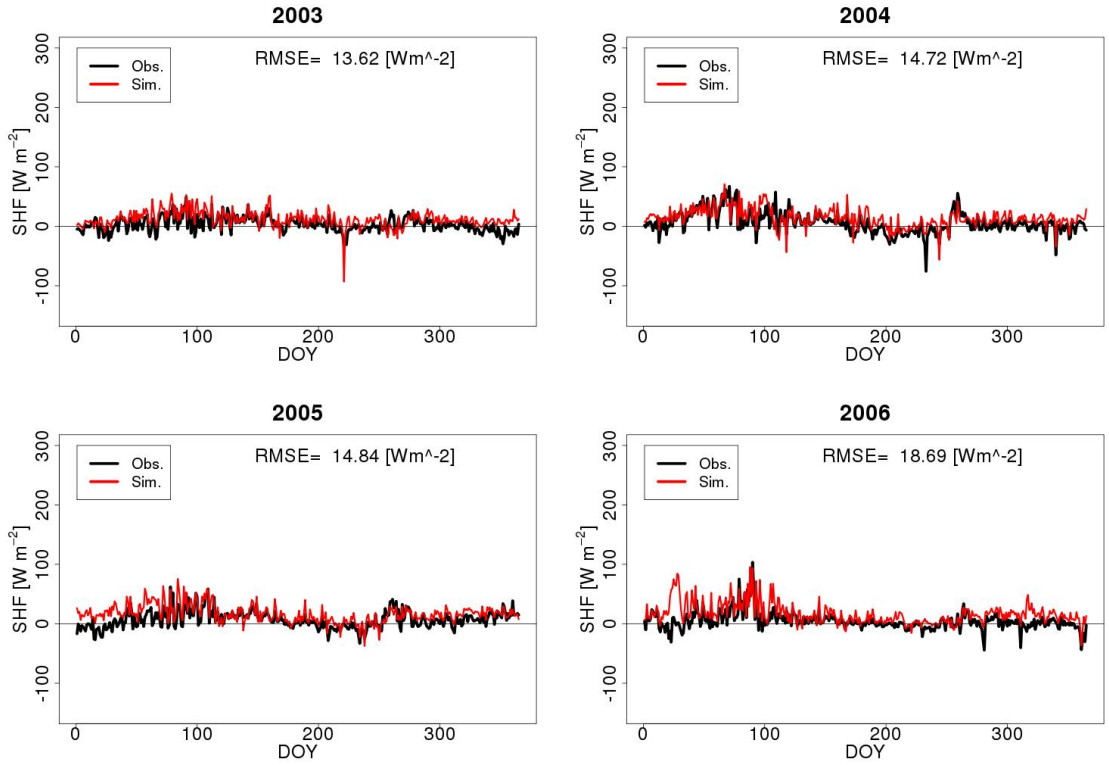

Figure 9. Comparison of sensible heat flux (SHF) between simulations and observations. DOY: The number of days from Jan. 1.

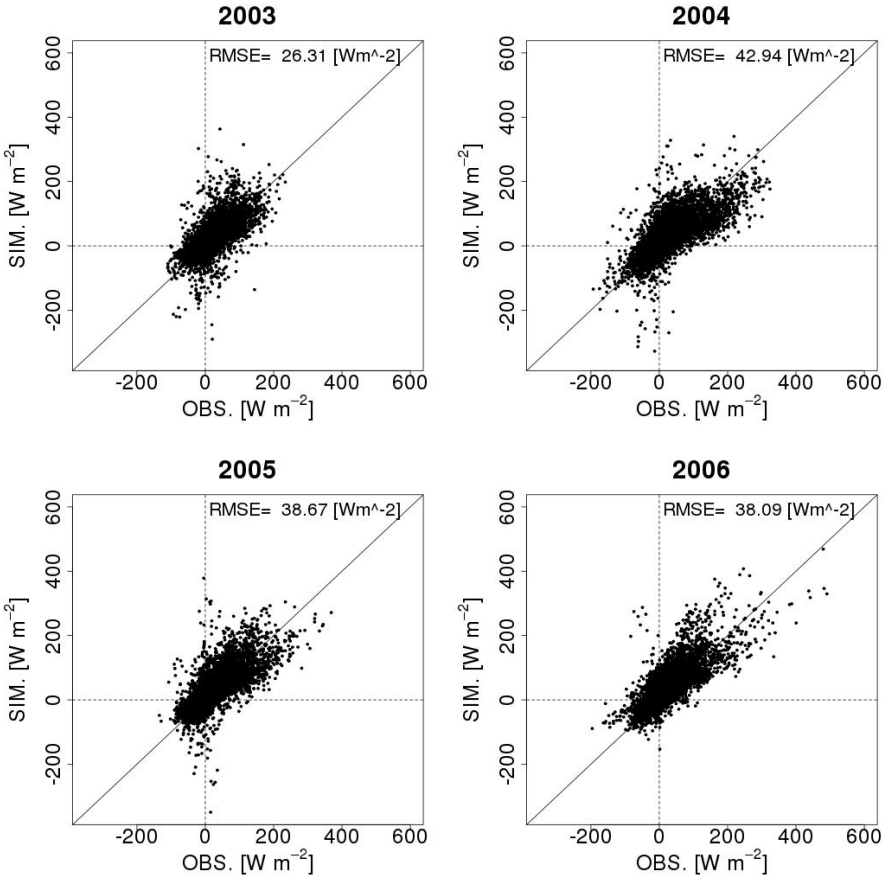

Figure 10. Comparison of half-hourly sensible heat flux (SHF) between simulations and observations.

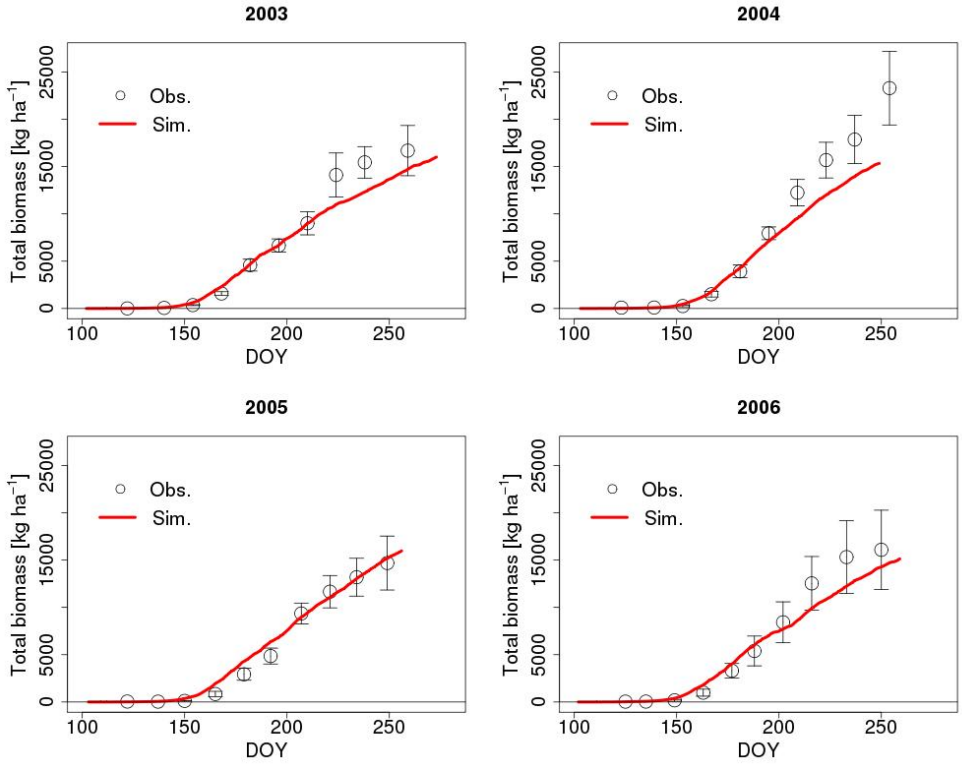

Figure 11. Comparison of total biomass between simulations and observations during growing periods from 2003 to 2006. Circles indicate mean values of observations and the ranges indicate standard deviation of observations. Red lines denotes simulations. DOY: The number of days from Jan. 1.

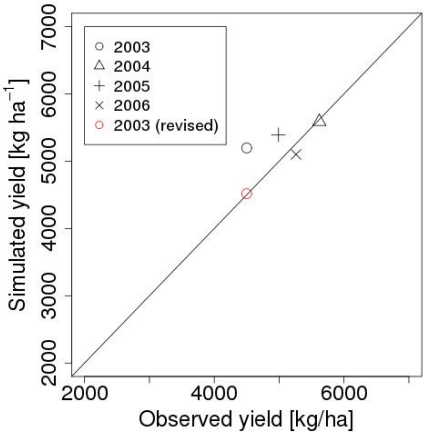

Figure 12. Comparison of yields between simulations and observations

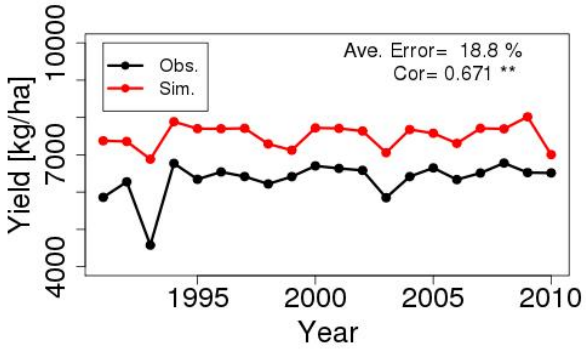

Figure 13. Comparison of yields over Japan between simulations and observations

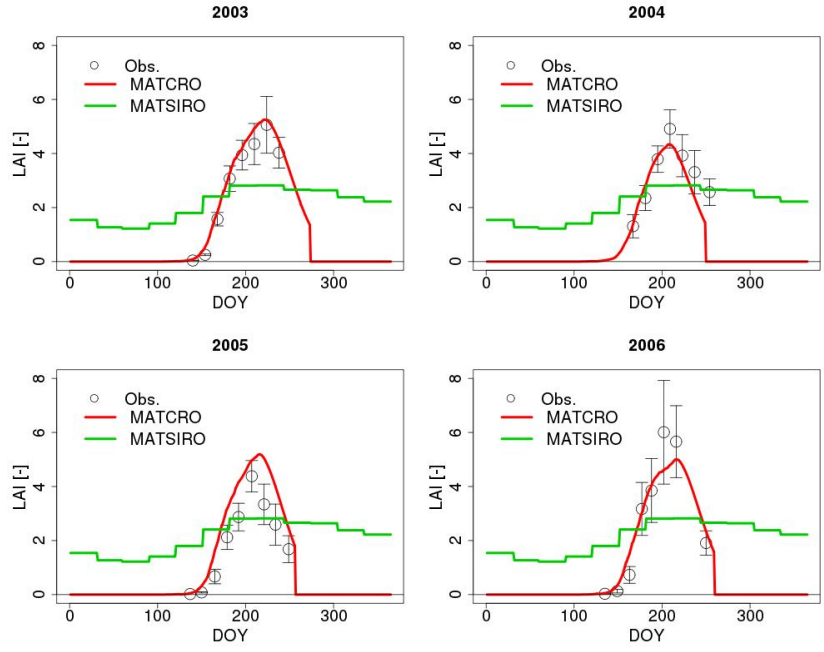

Figure 14. Comparison of LAI between observations, simulations by MATCRO, and the default value of MATSIRO

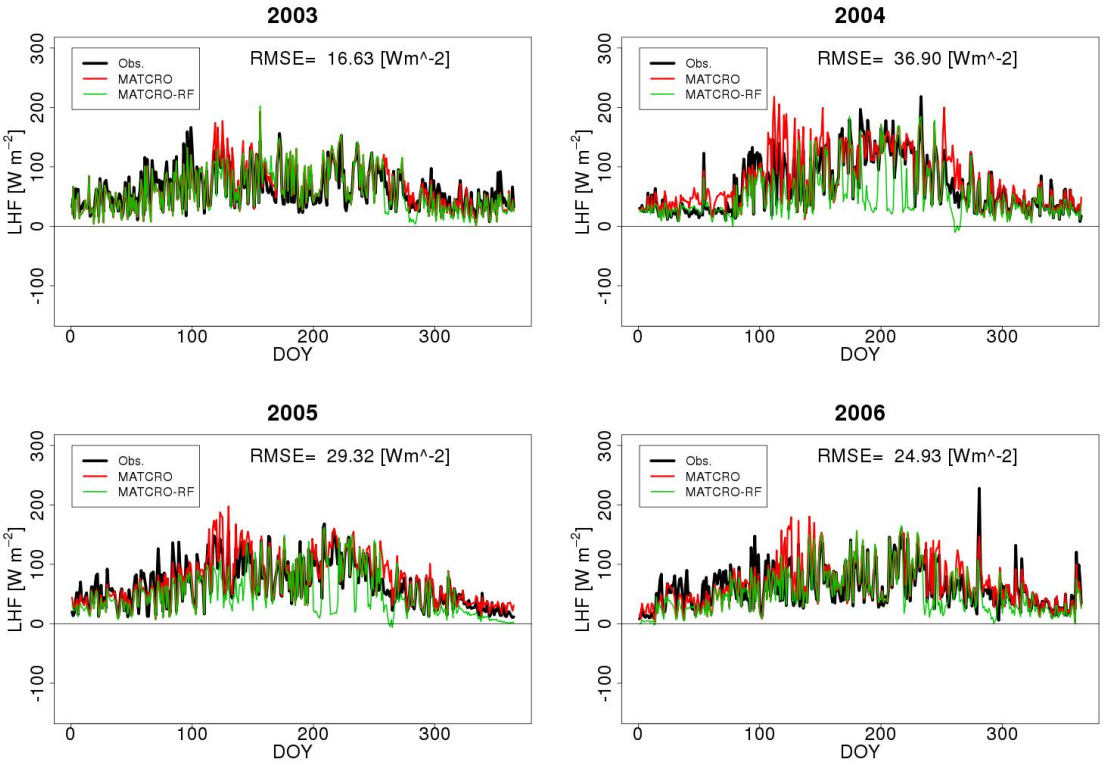

Figure 15. Comparison of daily latent heat flux (LHF) between observations and simulations by MATCRO and MATCRO-RF. DOY: The number of days from Jan. 1.

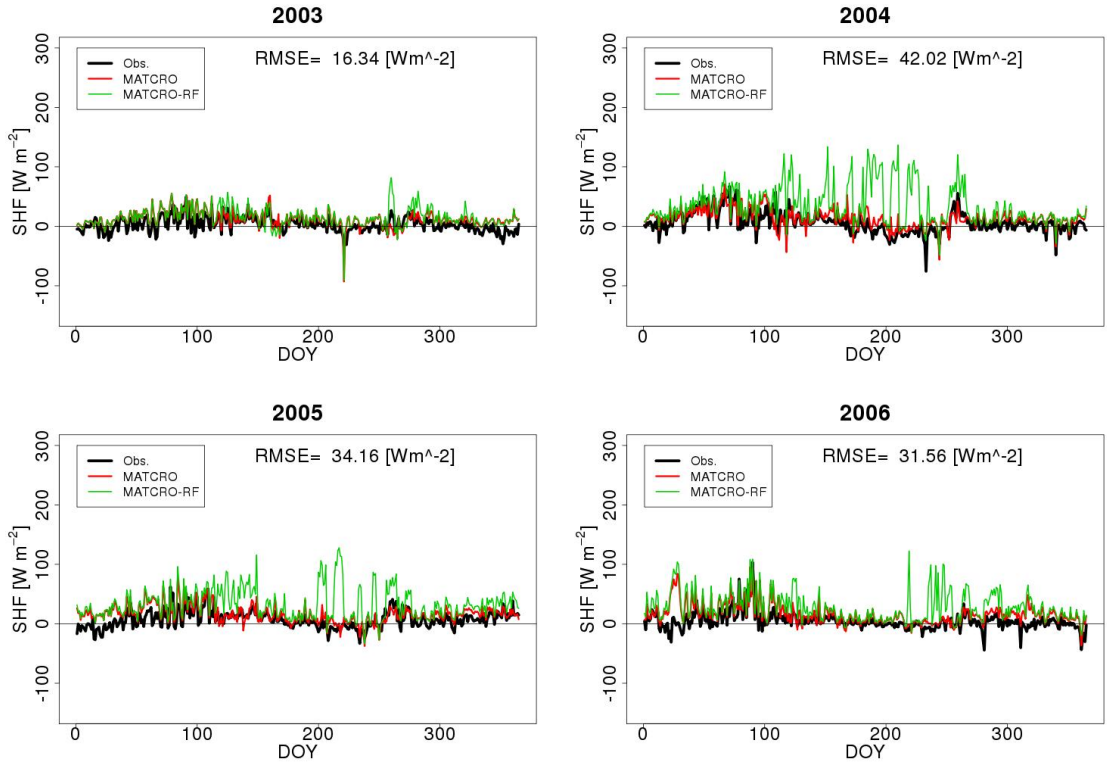

Figure 16. Comparison of sensible heat flux (SHF) between observation and simulations by MATCRO and MATCRO-RF. DOY: The number of days from Jan. 1.

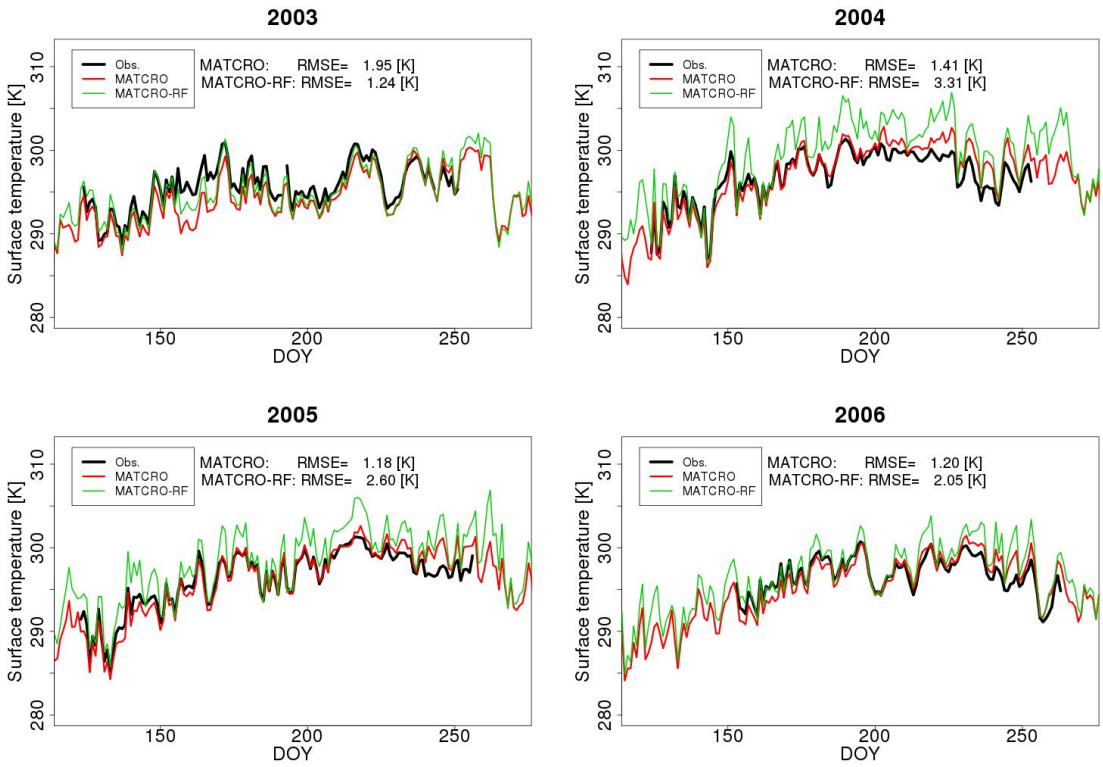

Figure 17. Surface temperature between observation and simulations by MATCRO and MATCRO-RF. DOY: The number of days from Jan. 1.

Table 1. Simulation setting parameters

Variable	Value	Unit	Description
$C_{\mathrm{a,ppm}}$	390	ppm	atmospheric CO_2 concentration
$D_{\mathrm{oy,Ie}}$	-	DOY	DOY of the day that irrigation and flooded surface end
$D_{\mathrm{oy,Is}}$	-	DOY	DOY of the day that irrigation and flooded surface start
$D_{\mathrm{oy,sw}}$	-	DOY	DOY of sowing day
d_{w}	0.025	m	depth of surface water
L_{t}	-	degree	latitude of the simulation site
$W_{\mathrm{glu},0}$	0.5	kg ha^{-1}	dry weight of glucose reserve at emergence
$W_{\mathrm{lef},0}$	1.0	kg ha^{-1}	dry weight of leaf at emergence
$W_{\mathrm{rot},0}$	1.0	kg ha^{-1}	dry weight of root at emergence
$W_{\mathrm{stm},0}$	1.0	kg ha^{-1}	dry weight of stem at emergence
z_{a}	3	m	reference height at which wind speed is observed
z_{max}	4	m	depth of soil layer
z_{t}	0.05	m	depth of top soil layer
z_{b}	2	m	depth from the soil surface to the upper bound of the bottommost layer of soil
δt	1800	s	time resolution

Table 2. Parameters parameterised

Variable	Value	Unit	Description
$D_{\mathrm{vs,rot1}}$	0.1	-	1st point of DVS at which the partition pattern to root changes
$D_{\mathrm{vs,rot2}}$	$D_{\mathrm{vs,h}}$	-	2nd point of DVS at which the partition pattern to root changes
$D_{\mathrm{vs,lef1}}$	0.2	-	1st point of DVS at which the partition pattern to leaf changes
$D_{\mathrm{vs,lef2}}$	0.7	-	2nd point of DVS at which the partition pattern to leaf changes
$D_{\mathrm{vs,pnc1}}$	0.5	-	1st point of DVS at which the partition pattern to panicle changes
$D_{\mathrm{vs,pnc2}}$	0.7	-	2nd point of DVS at which the partition pattern to panicle changes
$D_{\mathrm{vs,e}}$	0.012	-	DVS at emergence
f_{stc}	0.288	-	fraction of glucose allocated to starch reserves
h_{aa}	0.439	-	parameter for relationship between LAI and crop height before heading
h_{ab}	0.675	-	parameter for relationship between LAI and crop height before heading
h_{ba}	0.366	-	parameter for relationship between LAI and crop height after heading
h_{bb}	0.318	-	parameter for relationship between LAI and crop height after heading
$D_{\mathrm{vs,h}}$	0.616	-	DVS at heading
k_{yld}	0.675	-	ratio of crop yield to dry weight of panicle at maturity
$k_{\mathrm{S_{lw}}}$	3.5	-	parameter that represent the relationship between SLW and DVS
$G_{\mathrm{ds,m}}$	167759940	K· s	growing degree second at maturity
P_{rot}	0.25	-	partition ratio of glucose to root
P_{lef}	0.5	-	partition ratio of glucose to leaf from glucose partitioned to shoot
$r_{\mathrm{d1,lef}}$	5.0 * 10^{-7}	s^{-1}	ratio of leaf death at harvest
$S_{\mathrm{lw,mx}}$	600	kg m^{-2}	maximum specific leaf area
$S_{\mathrm{lw,mn}}$	350	kg m^{-2}	minimum specific leaf area
s_1	0.045	K^{-1}	temperature dependence of $\overline{V}_{max,x}$on $\overline{V}_{m,x}$
s_2	328	K	temperature dependence of $\overline{V}_{max,x}$ on $\overline{V}_{m,x}$
$V_{\mathrm{max}}(0)$	0.001	mol $\mathrm{m}^{-2}(l)$ s^{-1}	reference value for maximum Rubisco capacity at the canopy top
$D_{\mathrm{vs,tr}}$	0.06	-	DVS at transplanting and at which transplanting shock starts
$D_{\mathrm{vs,te}}$	0.08	-	DVS at which transplanting shock ends

Table 3. Observational data used for parameterisation

Variable	Unit	Description
L	$\mathrm{m}^2(l)\ \mathrm{m}^{-2}$	Leaf area index
$D_{\mathrm{oy,tr}}$	day	the number of days of transplanting from Jan. 1
$D_{\mathrm{oy,hd}}$	day	the number of days of heading from Jan. 1
$D_{\mathrm{oy,hv}}$	day	the number of days of harvest from Jan. 1
h_{gt}	m	Crop height
W_{lef}	kg ha^{-1}	dry matter weight of leaf
W_{stm}	kg ha^{-1}	dry matter weight of stem
W_{rot}	kg ha^{-1}	dry matter weight of root
W_{pnc}	kg ha^{-1}	dry matter weight of panicle
Y_{ld}	kg ha^{-1}	Yield

Table 4. Observational data used for validation at the parameterisation site

Variable	Unit	Description
Meteorological inputs		
P_{a}	Pa	Air pressure
P_{r}	kg m^{-2} s^{-1}	Precipitation
Q	kg kg^{-1}	Specific humidity
$R_{\mathrm{s}}^{\mathrm{d}}(0)$	W m^{-2}	Downward shortwave radiant flux density at the canopy top
$R_{\mathrm{l}}^{\mathrm{d}}(0)$	W m^{-2}	Downward longwave radiant flux density at the canopy top
T_{a}	K	Air temperature
U	m s^{-1}	Wind speed
$D_1^{\mathrm{d}}(0) + S_1^{\mathrm{d}}(0)$	W m^{-2}	Downward radiant flux density for photosynthesis active radiation at the canopy top
Management		
d_{wo}	m	Observed depth of surface water
$D_{\mathrm{oy,tr}}$	DOY	DOY of transplanting day
Outputs		
λE	W m^{-2}	Latent heat flux
H	W m^{-2}	Sensible heat flux
L	-	LAI
T_{g}	-	Surface temperature
$W_{\mathrm{sh}} + W_{\mathrm{rot}}$	kg ha^{-1}	Total biomass
Y_{ld}	kg ha^{-1}	Yield

Table 5. Soil-type specific parameters

Variable	Value	Unit	Description	Source
B	5.2	-	factor for hydraulic conductivity and water potential	Campbell and Norman (1998)
K_{s}	0.000064	kg s m^{-3}	hydraulic conductivity at saturation	Campbell and Norman (1998)
w_{sat}	0.48	m^3 m^{-3}	volumetric concentration of soil water at saturation	Saxton and Rawls (2006)
w_{wlt}	0.22	m^3 m^{-3}	volumetric concentration of soil water at wilting point	Saxton and Rawls (2006)
ψ_{s}	-2.6	J kg^{-1}	water potential at saturation	Campbell and Norman (1998)
ρ_{s}	1390	kg m^{-3}	bulk density of soil	Saxton and Rawls (2006)